Influence of chirality using Mn(III) salen complexes on DNA binding and antioxidant activity

Noor-ul H. Khan,*[a] Nirali Pandya,[a] Manoj Kumar,[b] Prasanta Kumar Bera,[a] Rukhsana I. Kureshy,[a] Sayed H. R. Abdi[a] and Hari C. Bajaj[a]

Received 16th April 2010, Accepted 24th June 2010
DOI: 10.1039/c0ob00010h

Chiral Mn(III) salen complexes ***S*-1**, ***R*-1**, ***S*-2**, ***R*-2**, ***S*-3** and ***R*-3** derived from the respective chiral salen ligands, *viz*., (1*S*,2*S*)-*N*,*N*′-bis-[3-*tert*-butyl-5-chloromethyl-salicylidine]-1,2-cyclohexanediamine ***S*-1′**/(1*R*,2*R*)-*N*,*N*′-bis-[3-*tert*-butyl-5-chloromethyl-salicylidine]-1,2-cyclohexanediamine ***R*-1′**/(1*S*,2*S*)-*N*,*N*′-bis-[3-*tert*-butyl-5-*N*,*N*′*N*′triethylaminomethyl-salicylidine]-1,2-cyclohexanediamine dichloride ***S*-2′**/(1*R*,2*R*)-*N*,*N*′-bis-[3-*tert*-butyl-5-*N*,*N*′*N*′triethylaminomethyl-salicylidine]-1,2-cyclohexanediamine dichloride ***R*-2′**/(1*S*,2*S*)-*N*,*N*′-bis-[3,5-di-*tert*-butylsalicylidene]-1,2-cyclohexanediamine ***S*-3′** and (1*R*,2*R*)-*N*,*N*′-bis-[3,5-di-*tert*-butyl-salicylidene]-1,2-cyclohexanediamine ***R*-3′**, were synthesized. Characterization of the complexes was done by microanalysis, IR, LC-MS, UV-vis. and circular dichroism (CD) spectroscopy. Binding of these complexes with calf thymus DNA (CT-DNA) was studied by absorption spectroscopy, competitive binding study, viscosity measurements, circular dichroism measurements, thermal denaturation study and observation of their different antioxidant activities. Among all the complexes used, the best result in terms of binding constant (intercalative) (130.4×10^4) was achieved with the complex ***S*-1** by spectroscopic titration. The complex ***S*-1** showed strong antioxidant activity as well.

Introduction

Chirality plays a significant role in medicinal chemistry because only one enantiomer of a drug molecule is likely to show desirable therapeutic effects while other enantiomer can have a different or adverse biological response. A classical example of this behavior was noticed in the use of thalidomide—a drug that was prescribed for morning sickness in pregnant women, where the ***R*** enantiomer showed drug action whereas ***S*** enantiomer caused birth defects.[1] Recently, the interaction of transition metal complexes with DNA evoked great interest, due to their importance in designing of new and promising drugs, probes for nucleic acids,[2–4] DNA-dependent electron transfer reactions, DNA footprinting, sequence-specific cleaving agents and antitumor drugs.[5–9] As DNA is chiral, its interaction with a molecule having a chiral center(s) is expected to be influenced by diastereomeric ion-pair formation between the two. Thus, different enantiomers of chiral metal complexes are expected to show different metallo-intercalation capacity with essentially chiral DNA and protein molecules.[10–16] As a consequence of this interaction, different enantiomers of a metal complex may have variable effects on various biological reactions, especially those involving free-radicals like hydrogen peroxide decomposition, superoxide anion (O_2^-) dismutase, catalase, water oxidation and ribonuclease reduction. These reactions are crucial for scavenging superoxide and hydroxyl radicals, which are largely responsible for DNA mutation and membrane protein damage that can lead to diseases like cancer, liver malfunction and cardiovascular problems.[17–19] Among various transition metal complexes, Mn(II)[20–22] and Mn(III) salen complexes[23] have shown promising results for the DNA binding and cleavage activity. Gravert and Griffin, in their exhaustive study on Mn(III) salen complexes, have demonstrated that the presence of substituents having different steric and electronic features on the salen moiety has a significant impact on their DNA binding/cleavage activity. They have also shown that in the case of chiral complexes (having no substituents on the salen moiety), different enantiomers have different DNA cleaving activity, the *R* enantiomer being more potent.[24] Recently, Peng *et al.* reported chiral Mn(III) salen complexes with a naphthaldehyde moiety for their potential DNA binding and cleavage activities.[20] However, in this study the difference in DNA binding/cleavage activity between the two enantiomers was found to be less pronounced. These results clearly demonstrated that the DNA binding and cleavage activity of the Mn(III) salen complexes is strongly substituent dependent. However, Melvo *et al.* elegantly demonstrated the superoxide scavenging antioxidant activity of Mn salen complexes utilizing achiral ligands by xanthine–xanthine oxidase assay.[25] Ironically, the role of chirality on superoxide and hydrogen peroxide radical scavenging activities is conspicuously absent.

In view of the above and our ongoing interest in the synthesis of various chiral transition metal complexes as catalysts in various organic transformations[26–29] and DNA binding and cleavage studies,[11] here, we are reporting the synthesis of chiral Mn(III) salen complexes, *viz*. ***S*-1**, ***R*-1**, ***S*-2**, ***R*-2**, ***S*-3** and ***R*-3**, having different substituents such as chloromethyl, triethylaminomethyl and *tert*-butyl at the 5,5′-position of salen and examined their

[a]*Discipline of Inorganic Materials and Catalysis, Central Salt and Marine Chemicals Research Institute (CSMCRI), Council of Scientific & Industrial Research (CSIR), G. B. Marg, Bhavnagar-364 021, Gujarat, India. E-mail: khan251293@yahoo.in; Fax: +91-0278-2566970; Tel: +91-0278 2567760*
[b]*Marine Biology and Ecology Discipline, Central Salt and Marine Chemicals Research Institute (CSMCRI), Council of Scientific & Industrial Research (CSIR), G. B. Marg, Bhavnagar-364 021, Gujarat, India; Fax: +91-0278-2566970; Tel: +91-0278 2567760*

activity in calf thymus DNA (CT-DNA) binding by absorption spectroscopy, competitive binding study, viscosity measurements, CD measurements and thermal denaturation studies. We have also evaluated, for the first time, the role of the chirality of these complexes on antioxidant activity, *e.g.*, DPPH, superoxide and hydrogen peroxide radical scavenging activity. Among the complexes studied here, the ***S*-1** enantiomer of the Mn(III) salen complex showed highest DNA intercalation capacity and ~95% free radical inhibition activity, whereas its other enantiomer, ***R*-1** exhibited groove binding or external binding with DNA and 69% free radical inhibition activity.

Results and discussion

Chiral salen complexes, *viz*., (1*S*,2*S*)-*N*,*N*′-bis-[3-*tert*-butyl-5-chloromethyl-salicylidine]-1,2-cyclohexanediaminato manganese-(III) chloride ***S*-1**/(1*R*,2*R*)-*N*,*N*′-bis-[3-*tert*-butyl-5-chloromethyl-salicylidine]-1,2-cyclohexanediaminato manganese(III) chloride ***R*-1**/(1*S*,2*S*)-*N*,*N*′-bis-[3-*tert*-butyl-5-*N*,*N*′*N*′triethylaminomethyl-salicylidine]-1,2-cyclohexanediaminato manganese(III) trichloride ***S*-2**/(1*R*,2*R*)-*N*,*N*′-bis-[3-*tert*-butyl-5-*N*,*N*′*N*′triethylaminomethyl-salicylidine]-1,2-cyclohexanediaminato manganese-(III) trichloride ***R*-2**/(1*S*,2*S*)-*N*,*N*′-bis-[3,5-di-*tert*-butylsalicylidene]-1,2-cyclohexanediaminato manganese(III) chloride ***S*-3** and (1*R*,2*R*)-*N*,*N*′-bis-[3,5-di-*tert*-butyl-salicylidene]-1,2-cyclohexanediaminato manganese(III) chloride ***R*-3** were prepared by the interaction of their respective chiral salen ligands,[30–33] with manganese(II) acetate under an inert atmosphere followed by addition of LiCl under aerobic condition (Scheme 1). All the chiral metal complexes were characterized by microanalysis, IR, LC-MS, UV-vis. and CD spectroscopy (data given in the experimental section).

DNA binding and antioxidant activity

Electronic absorption spectroscopy was used to study the interaction of metal complexes ***S*-1**, ***R*-1**, ***S*-2**, ***R*-2**, ***S*-3** and ***R*-3**

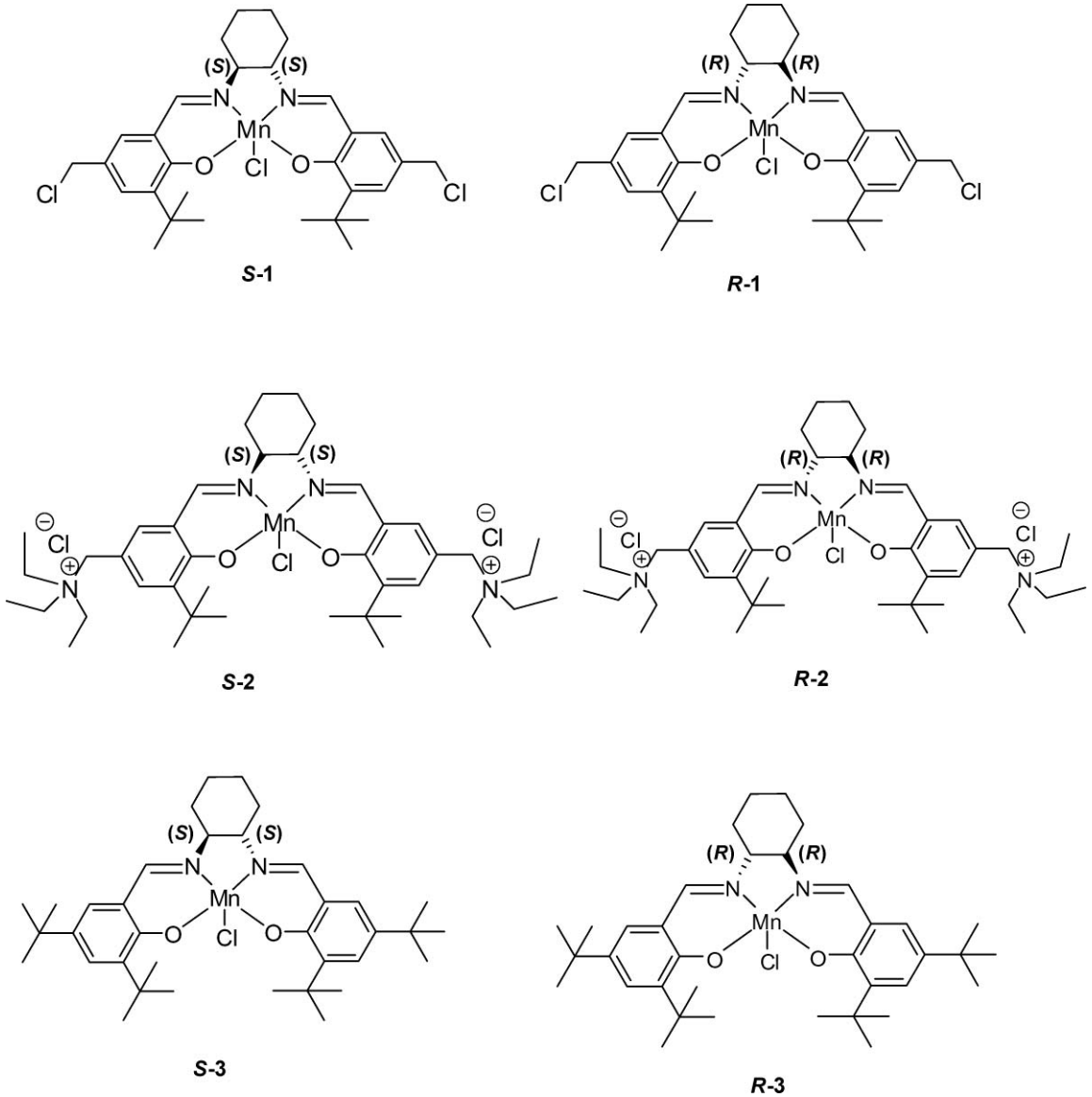

Scheme 1 Structure of chiral Mn(III) salen complexes.

with DNA. The change in absorbance and shift in wavelength upon addition of increasing concentrations of DNA solution in a fixed concentration of chiral metal complexes gives valuable information on the mode of interaction. The metal complex binding with DNA through intercalation usually results in hypochromism and bathochromism due to the strong stacking interaction between the aromatic chromophore and the base pairs of DNA.[34] The absorption spectra of chiral Mn(III) salen complexes ***S*-1**, ***R*-1**, ***S*-2**, ***R*-2**, ***S*-3** and ***R*-3** with DNA are shown in Fig. 1, 2 and 3. Upon increasing the concentration of CT-DNA in the solution of the complexes ***S*-1** and ***R*-1**, the bands at 318 and 400 nm showed hypochromism while complexes ***S*-2** and ***R*-2** showed hyperchromism for the 325 and 411 nm bands. Interestingly, complexes ***S*-3** and ***R*-3** showed both hypochromism

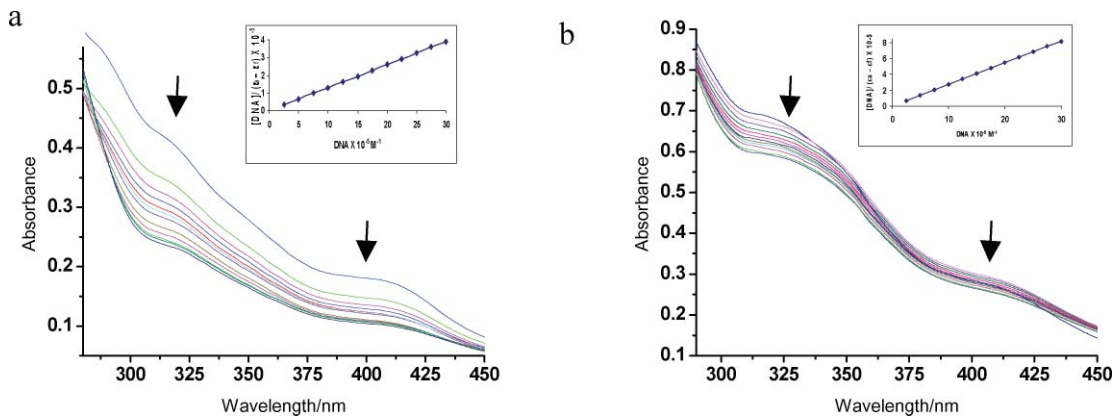

Fig. 1 Absorption spectra of chiral Mn(III) salen complexes (50 μM) (a) ***S*-1** (b) ***R*-1** in phosphate buffer (1 mM, pH 7.0) in the presence of increasing concentrations of DNA. DNA = 0–300 μM. Inset plot is $[DNA]/(\varepsilon_a - \varepsilon_f)$ *vs.* DNA.

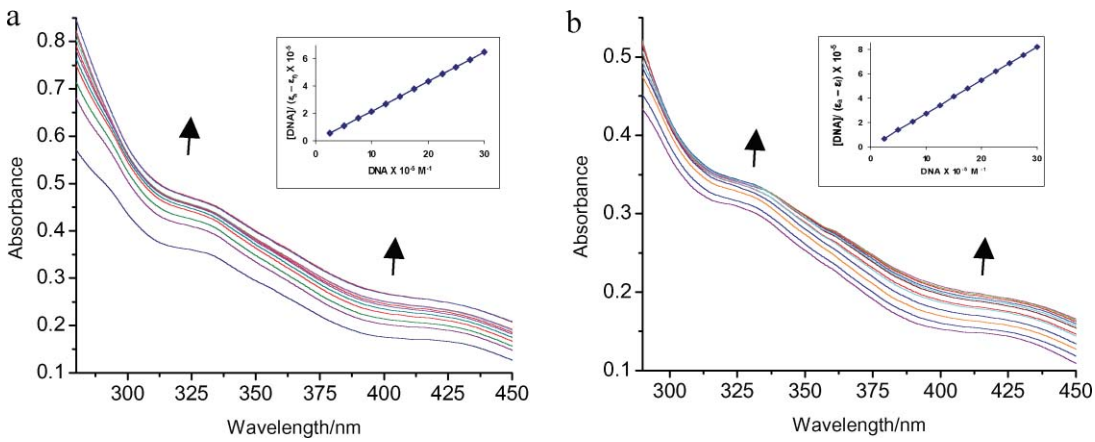

Fig. 2 Absorption spectra of chiral Mn(III) salen complexes (50 μM) (a) ***S*-2** (b) ***R*-2** in phosphate buffer (1 mM, pH 7.0) in the presence of increasing concentrations of DNA. DNA = 0–300 μM. Inset plot is $[DNA]/(\varepsilon_a - \varepsilon_f)$ *vs.* DNA.

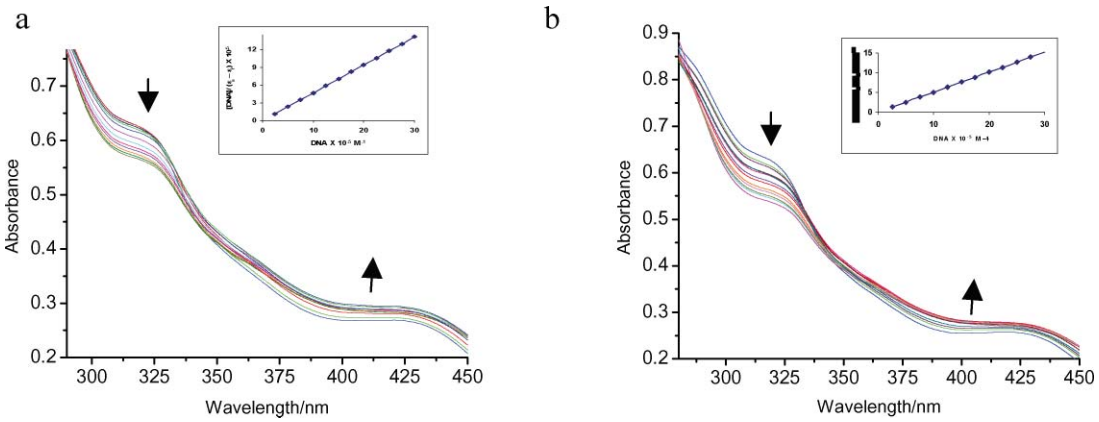

Fig. 3 Absorption spectra of chiral Mn(III) salen complexes (50 μM) (a) ***S*-3** (b) ***R*-3** in phosphate buffer (1 mM, pH 7.0) in the presence of increasing concentrations of DNA. DNA = 0–300 μM. Inset plot is $[DNA]/(\varepsilon_a - \varepsilon_f)$ *vs.* DNA.

and hyperchromism for the 315 nm and 415 nm bands, respectively. These spectroscopic characteristics suggest that all the chiral Mn(III) salen complexes tested had some interaction with DNA. Among these, complex ***S*-1** showed strongest interaction.[21,35]

The intrinsic binding constant of all the complexes with DNA was obtained by monitoring the changes in absorbance of the LMCT band of complexes with increasing concentration of DNA using the following functional equation.

$$[DNA]/(\varepsilon_a - \varepsilon_f) = [DNA]/(\varepsilon_b - \varepsilon_f) + 1/K_b(\varepsilon_b - \varepsilon_f) \quad (1)$$

Where [DNA] is the concentration of DNA in base pairs, ε_a, ε_f and ε_b correspond to A_{obs}/[Mn], the extinction coefficient of the free chiral Mn(III) salen complex, and the extinction coefficient of the chiral Mn(III) salen complex in the fully bound form, respectively. K_b was obtained from the ratio of the slope to intercept by using the plot of $[DNA]/(\varepsilon_a - \varepsilon_f)$ *vs.* [DNA] (Table 1). The results in Table 1 indicate that more polar complexes ***S*-1**, ***R*-1**, ***S*-2** and ***R*-2** bind quite strongly with DNA due to the presence of chloromethyl and triethylaminomethyl groups at the 5 and 5′ positions of these complexes. On the other hand complexes ***S*-3** and ***R*-3**, which bear hydrophobic groups (*tert*-butyl) at these locations bind relatively less strongly with DNA. Further, among complexes ***S*-1**, ***R*-1**, ***S*-2**, ***R*-2**, ***S*-3** and ***R*-3** the ***S*** enantiomer of the complexes bind more strongly than their ***R*** counterparts, however, the complex ***S*-1** showed strong binding through intercalation while ***R*-1**, ***S*-2**, ***R*-2**, ***S*-3** and ***R*-3** bind through groove or external binding with DNA. These results are significantly superior as compared to the earlier report[20] where different aldehyde moieties on Mn(III) salen complexes with no substituents on the catalyst were used for DNA binding studies, which gives K_b for the ***R*** enantiomer as $(1.26 \pm 0.12) \times 10^4$ M^{-1} and the ***S*** enantiomer as $(1.09 \pm 0.13) \times 10^4$ M^{-1}.

Table 1 Binding constant of ***S*** and ***R*** enantiomers of chiral Mn(III) salen complexes

Entry	Complexes	λ_{max}/nm	$K_b \times 10^4 \pm 0.01$ M^{-1}
1	***S*-1**	318, 400	130.4
2	***R*-1**	318, 400	27.3
3	***S*-2**	325, 411	52.17
4	***R*-2**	325, 411	27.3
5	***S*-3**	315, 415	15.7
6	***R*-3**	315, 415	12.6

Luminescence spectroscopy study

Chiral Mn(III) salen complexes ***S*-1**, ***R*-1**, ***S*-2**, ***R*-2**, ***S*-3** and ***R*-3** show no luminescence upon excitation of the CT and LMCT bands, irrespective of the presence or absence of a solvent or CT-DNA. Hence, competitive binding studies for these complexes was carried out by fluorescence spectral method using the emission intensity of ethidium bromide (EB) as a probe. In control experiments, when chiral metal complex solutions of increasing concentration were added to ethidium bromide solution, there was no change in the emission intensity of EB in the absence of DNA, indicating that there is no interaction between the EB and the complex. EB is known to emit intense fluorescence in the presence of DNA due to the strong intercalation between the base pairs of DNA. It has been reported that the enhanced fluorescence can be quenched by the addition of the second molecule.[11,36] In the present study it can be clearly seen from Fig. 4, 5 and 6 that there is a reduction in the emission intensity of the DNA-bound EB on the addition of increasing concentrations of chiral Mn(III) salen complexes suggesting its competitive binding with DNA–EB.

Based on the above data, the Stern–Volmer quenching constant can be calculated by using the following equation

$$I_0/I = 1 + Kr \quad (2)$$

In the above equation I_0 and I are the emission intensities in the absence and presence of chiral Mn(III) salen complexes and r is the ratio of the total concentration of chiral complexes to DNA. Accordingly, the plot Fig. 7 of I_0/I *vs.* [Mn]/[DNA], K is given by the ratio of the slope to intercept.

The K values thus calculated (Table 2) suggest that the $\Delta\lambda$/nm and Stern–Volmer constant values are highest for ***S*-1**. However, in general, the ***S*** enantiomer showed stronger binding with DNA than the ***R*** enantiomer, suggesting that the DNA, which is essentially chiral in nature, indeed shows a stereochemical preference for binding with external chiral molecules and is also affected by the steric and electronic properties of the complexes.

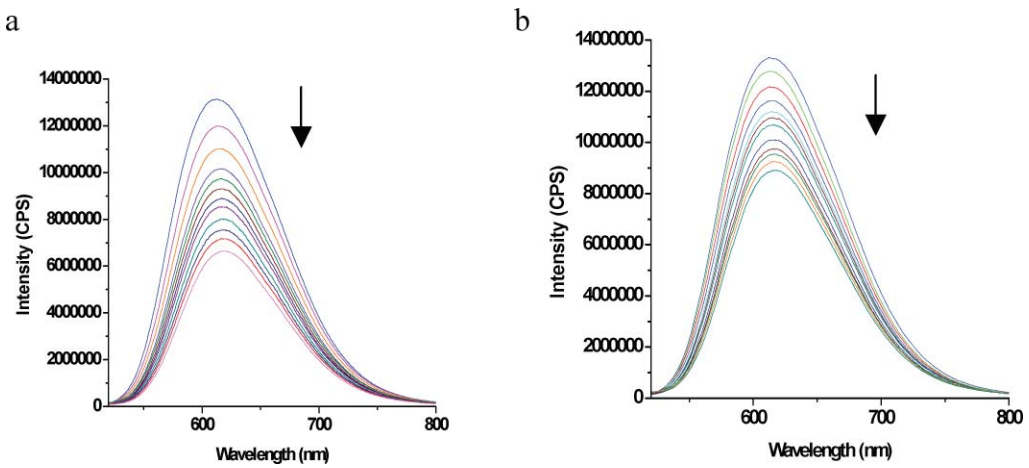

Fig. 4 The emission spectra of DNA-bound EB in the presence of (a) ***S*-1** (b) ***R*-1** in phosphate buffer (1 mM, pH 7.0) in the presence of increasing concentration of the complexes. DNA = 100 μM.

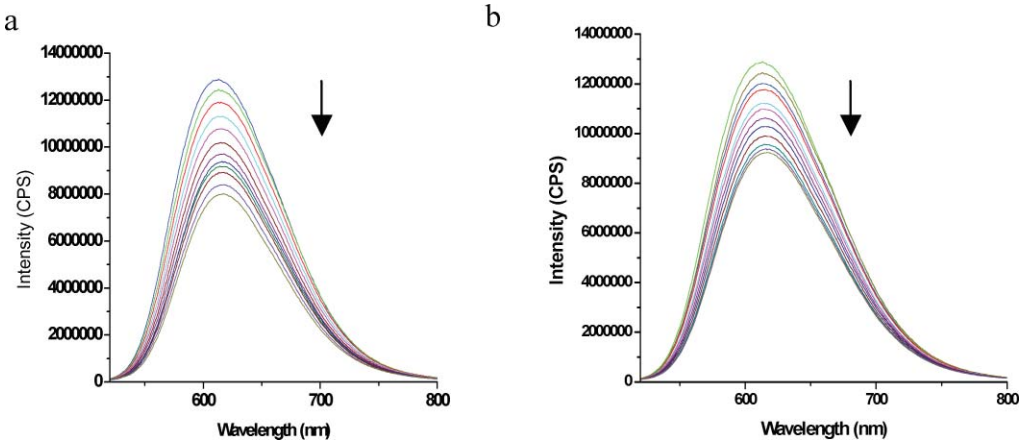

Fig. 5 The emission spectra of DNA-bound EB in the presence of (a) ***S*-2** (b) ***R*-2** in phosphate buffer (1 mM, pH 7.0) in the presence of increasing concentration of the complexes. DNA = 100 μM.

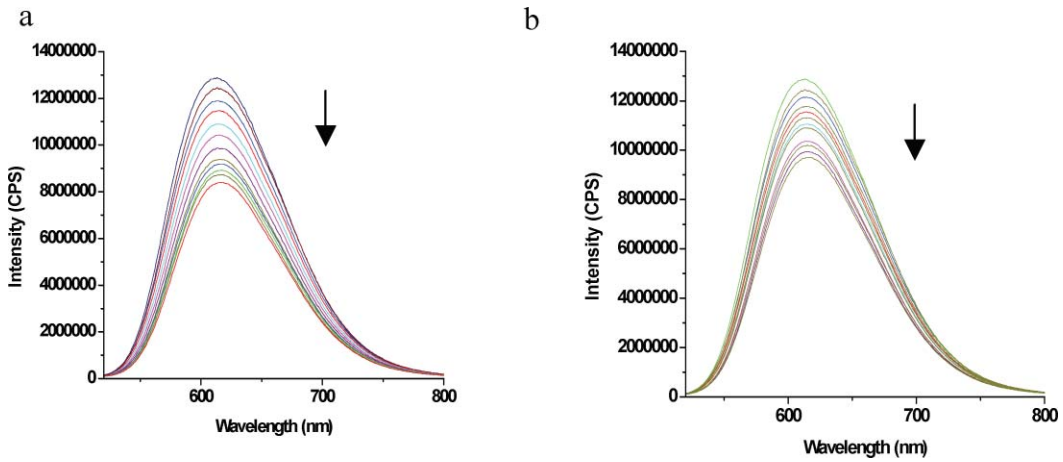

Fig. 6 The emission spectra of DNA-bound EB in the presence of (a) ***S*-3** (b) ***R*-3** in phosphate buffer (1 mM, pH 7.0) in the presence of increasing concentration of the complexes. DNA = 100 μM.

Table 2 Stern–Volmer constant of ***S*** and ***R*** enantiomers of chiral Mn(III) salen complexes

Complexes	λ_{max}, DNA + EB	λ_{max}, DNA + EB + complex	$\Delta\lambda$/nm	K
***S*-1**	612	620	8	0.77 ± 0.012
***R*-1**	612	616	4	0.41 ± 0.013
***S*-2**	612	617	5	0.49 ± 0.01
***R*-2**	612	616	4	0.39 ± 0.017
***S*-3**	612	616	4	0.51 ± 0.009
***R*-3**	612	615	3	0.30 ± 0.013

Hence, among all the complexes studied, complex ***S*-1** binds with DNA more efficiently through intercalation, while the complexes ***R*-1**, ***S*-2**, ***R*-2**, ***S*-3** and ***R*-3** either bind through groove or external binding with DNA. These results are in consonance with the electronic absorption titration studies given earlier in the section.

Circular dichroism spectroscopy

The CD spectral analysis is a powerful tool which gives valuable information on the binding mode of chiral metal complexes with DNA.[16,20] The CD spectra of complexes ***S*-1**, ***R*-1**, ***S*-2**, ***R*-2**, ***S*-3** and ***R*-3** in DMSO are shown in Fig. 8, 9 and 10. The CD spectra of free ***S*-1**, ***S*-2** and ***S*-3** and their respective enantiomers ***R*-1**, ***R*-2** and ***R*-3** show bands of opposite configuration at ~320 and ~415 nm. Complexes ***S*-1** and ***R*-1** showed increases in spectral strength of 32% on interaction with CT-DNA in the CT region, whereas the LMCT band of ***S*-1** had a red shift of 3 nm in the presence of CT-DNA with an increase in spectral strength by 26%. On the contrary, the LMCT band of ***R*-1** showed a decrease in spectral strength by 21% with a 1 nm blue shift. These results clearly indicate the different matching of enantiomers of the complex with DNA. On the other hand, complex ***S*-2** in the presence of DNA showed a blue shift of 1 nm in the LMCT region with a decrease in spectral strength (23%), while ***R*-2** showed an increase in spectral strength (22%) with a blue shift of 1 nm in this region. Paradoxically, complexes ***S*-3** and ***R*-3** showed no significant change in the CD spectra in the presence of DNA. These results show that both substituents at the 5,5′-position on the salen moiety and the chirality of the complexes used in the present study have profound effects on the binding efficiency with DNA.

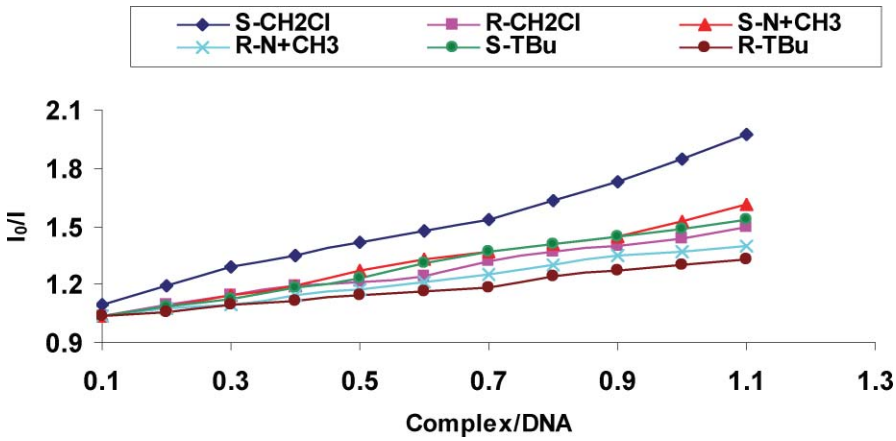

Fig. 7 Fluorescence quenching curve of DNA-bound EB of chiral Mn(III) salen complexes, [EB] = 30 μM, [DNA] = 100 μM, [chiral ***S*** and ***R*** enantiomers of Mn(III) salen complexes] = 0–110 μM.

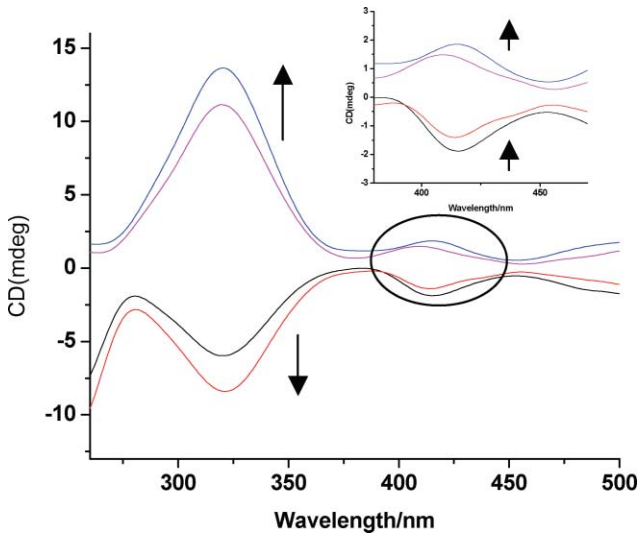

Fig. 8 CD spectra of chiral Mn(III) salen complexes ***S*-1** and ***R*-1** in the presence and absence of DNA. Complex concentration = 50 μM. Inset graph shows changes in the presence of CT-DNA in the LMCT region.

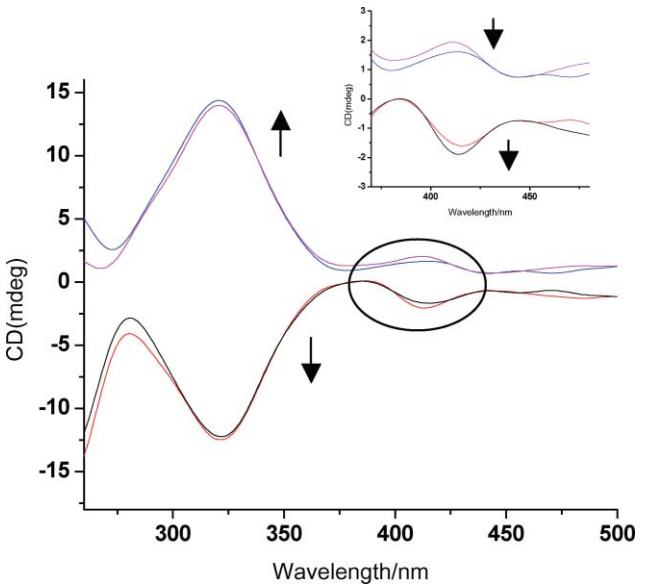

Fig. 9 CD spectra of chiral Mn(III) salen complexes ***S*-2** and ***R*-2** in the presence and absence of DNA. Complex concentration = 50 μM. Inset graph shows changes in the presence of CT-DNA in the LMCT region.

Viscosity study

To further strengthen our understanding of the interactions of chiral Mn(III) salen complexes ***S*-1**, ***S*-2**, ***S*-3**, ***R*-1**, ***R*-2**, ***R*-3** with DNA, viscosity measurements were carried out. Hydrodynamic measurements that are sensitive to length change are regarded as the least ambiguous and most critical test of binding mode in the absence of crystallographic structural data.[11,36,37]

A partial and non-classical intercalation ligand could bend the DNA helix, thereby reducing its effective length and its viscosity. On the contrary, a classical intercalation model often causes lengthening of the DNA helix, as base pairs are separated to accommodate the binding ligand, leading to the increase in DNA viscosity. Fig. 11 shows the changes in relative viscosity of CT-DNA in the presence of ***S*** and ***R*** enantiomers of chiral Mn(III) salen complexes. The results clearly show that the complex ***S*-1** induced the maximum increase in the density, indicating strong intercalative binding between the base pairs of DNA as against its enantiomer ***R*-1**. A similar trend of increases in density was also observed with complexes ***S*-2** and ***R*-2**, although the extent of binding was less. However, complexes ***S*-3** and ***R*-3** showed no significant increase in density, possibly due to poor binding with DNA. Thus, overall binding affinity to DNA follows the order of ***S*-1** > ***R*-1** > ***S*-2** > ***S*-3** > ***R*-2**> ***R*-3**.

Thermal denaturation study

The thermal behavior of DNA in the presence of complexes can give an insight into their conformational changes and also information about the interaction affinity of complexes. It is well known that on increasing the temperature, the double stranded DNA shows hyperchromism due to its gradual dissociation to form single strands. The melting curves of CT-DNA in the presence and absence of the chiral Mn(III) salen complexes are shown in Fig. 12.

The T_m of CT-DNA was found to be 70 °C in the absence of a complex. The T_m of the CT-DNA in the presence of ***S*-1** increased

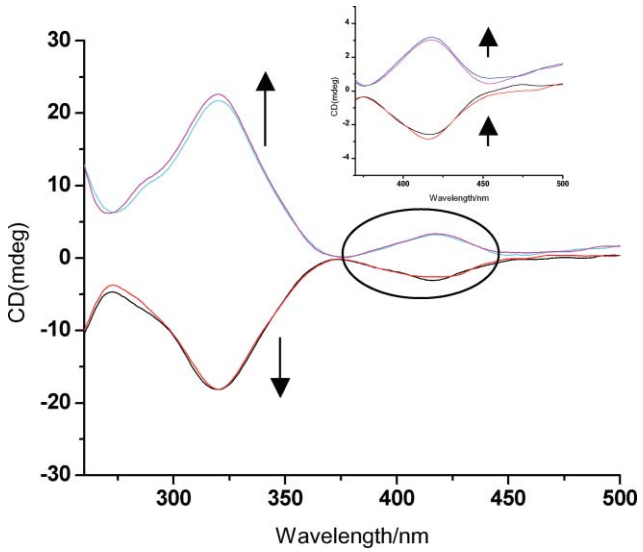

Fig. 10 CD spectra of chiral Mn(III) salen complexes ***S*-3** and ***R*-3** in the presence and absence of DNA. Complex concentration = 50 μM. Inset graph shows changes in the presence of CT-DNA in the LMCT region.

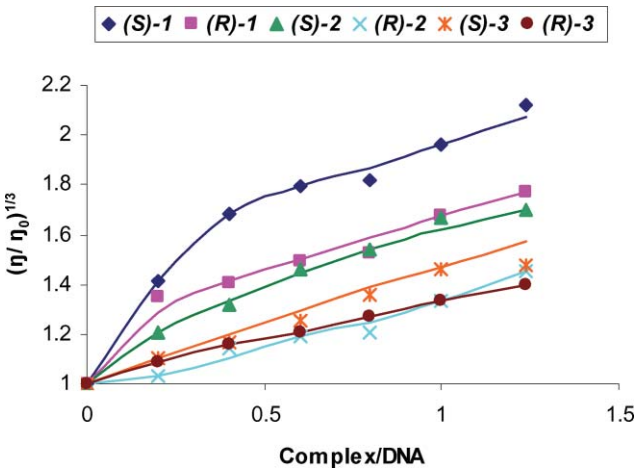

Fig. 11 The relative viscosity of DNA (50 μM) in the presence of chiral ***S*** and ***R*** enantiomers of Mn(III) salen complexes (0–60 μM).

to 75 °C showing retardation in the dissociation of the DNA helix due to strong binding with the metal complex. Other complexes, *e.g.*, ***R*-1**, ***S*-2**, ***R*-2** and ***S*-3** do not alter the T_m value of CT-DNA, which remains at 70 °C. On the contrary, ***R*-3** showed a decrease in T_m value (65 °C) of CT-DNA, possibly due to its instability in the presence of this complex. Based on the above observations, it can be concluded that ***S*-1** binds with DNA through intercalation whereas ***R*-1**, ***S*-2**, ***R*-2**, ***S*-3** and ***R*-3** had groove or external binding with DNA.

Antioxidant activity

DPPH radical scavenging activity. DPPH is a stable free radical, which has been widely used to estimate the radical scavenging activity of antioxidants.[38] Generally, it has the ability to accept an electron or hydrogen radical to become a stable diamagnetic molecule. Thus, it shows a decrease in absorbance at 517 nm whose intensity depends on the number of electrons it has taken up. DPPH radical scavenging activity for ***S*-1**, ***R*-1**, ***S*-2**, ***R*-2**, ***S*-3** and ***R*-3** was found to be 95, 67, 74, 50, 59 and 56% at 20 μM concentration, respectively (Fig. 13). These results indicate some correlation between DNA binding ability as described in the preceding sections and free radical scavenging activity. The complex ***S*-1** that showed the strongest DNA binding ability has also demonstrated the highest DPPH radical scavenging activity. This study has further strengthened the fact that for the present set of complexes, the ***S*** enantiomer is more effective than their ***R*** counterpart.

Superoxide and hydrogen peroxide radical scavenging activity

Superoxide ($O_2^{\bullet -}$) and hydrogen peroxide (H_2O_2) are highly reactive compounds among the reactive oxygen species (ROS).

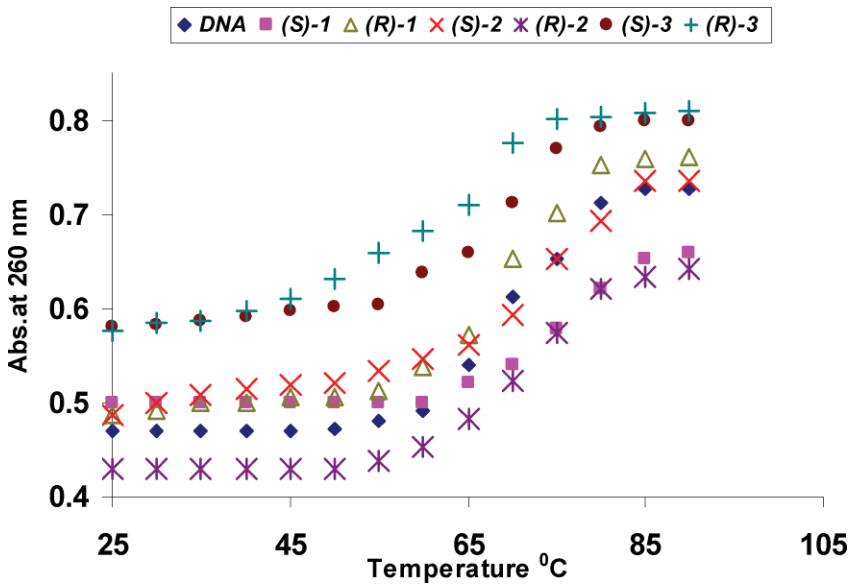

Fig. 12 Thermal denaturation graph of CT-DNA (0.4 mM) in the presence of chiral ***S*** and ***R*** enantiomers of Mn(III) salen complexes (20 μM).

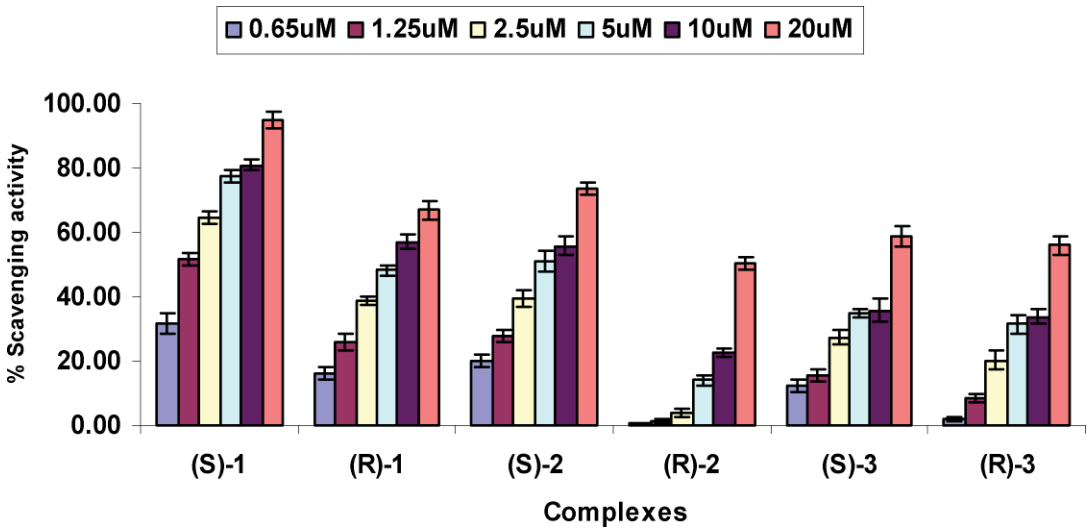

Fig. 13 DPPH scavenging effect by ***S*-1**, ***R*-1**, ***S*-2**, ***R*-2**, ***S*-3** and ***R*-3** chiral Mn(III) salen complexes.

These species can disintegrate cell membranes and damage protein and DNA structures and are largely responsible for many diseases, such as cancer, liver injury and cardiovascular complications.[17] A few manganese complexes have been reported earlier to show anti-ROS activity,[39–44] however, to the best of our knowledge there is no report on the role of chirality in the disintegration of ROS ($O_2^{\bullet-}$ and H_2O_2). In the present study we have tried to examine the antioxidant potential of different enantiomers of chiral Mn(III) salen complexes. As shown in Fig. 14, the superoxide radical scavenging abilities of the test chiral Mn(III) salen complexes increased with the increasing concentration of the complexes ranging from 0.65–20 μM. In the superoxide radical scavenging activity, the chiral Mn(III) salen complexes capable of oxidizing $O_2^{\bullet-}$ anion will compete with NBT and slow down its reduction, *i.e.* formation of blue formazon color, and thus, decreases the absorbance at 560 nm. The results shown in Fig. 14 clearly indicate the highest superoxide scavenging behavior for the complex ***S*-1** with 81% scavenging effect, as compared to ***R*-1** with 57% at a concentration of 20 μM. Complexes ***S*-2** and ***R*-2** also showed a high scavenging activity with 60% and 51%, respectively. In contrast, the complexes ***S*-3** and ***R*-3** having *tert*-butyl groups at the 3,3′ and 5,5′ positions showed almost negligible scavenging activity at all concentrations tested. These results indicate that the complex ***S*-1** showed highest superoxide scavenging activity. Similar results were also observed for H_2O_2 scavenging for the test chiral Mn(III) salen complexes, ***S*-1**, ***R*-1**, ***S*-2**, ***R*-2**, ***S*-3** and ***R*-3** (Fig. 15). ***S*-1** and ***S*-2** were found to be potential scavengers of H_2O_2 with 82% and 74% scavenging ability, respectively. In contrast, other chiral Mn(III) salen complexes, namely ***R*-1**, ***R*-2**, ***S*-3** and ***R*-3** gave 45, 34, 45 and 38% scavenging activity, respectively, at a concentration of 20 μM. In all the cases it is clear from the results that the ***S*** enantiomers of the complexes are more active than their respective ***R*** enantiomers. This trend is probably due to the fact that the ***S*** enantiomer of the complexes used in the present

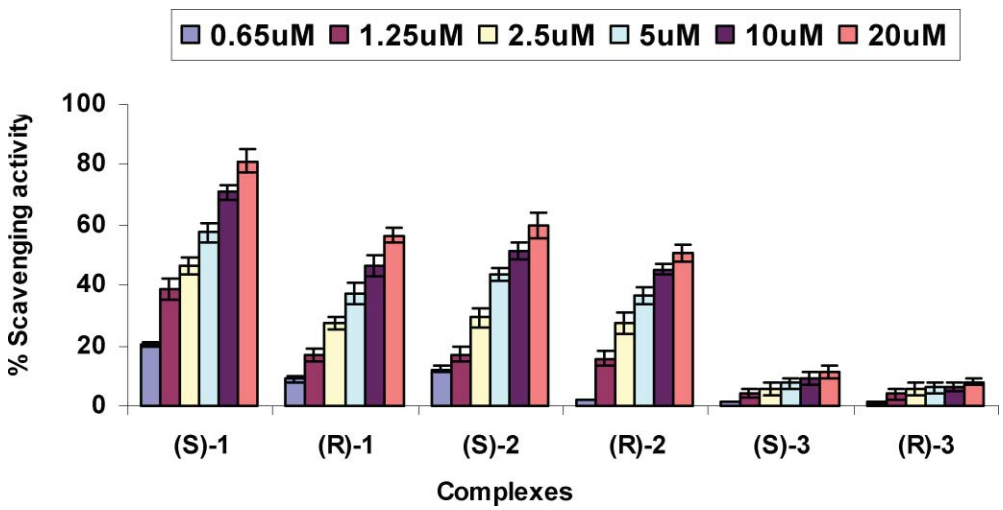

Fig. 14 Scavenging effect of the chiral Mn(III) salen complexes on $O_2^{\bullet-}$ by MET/VitB2/NBT system.

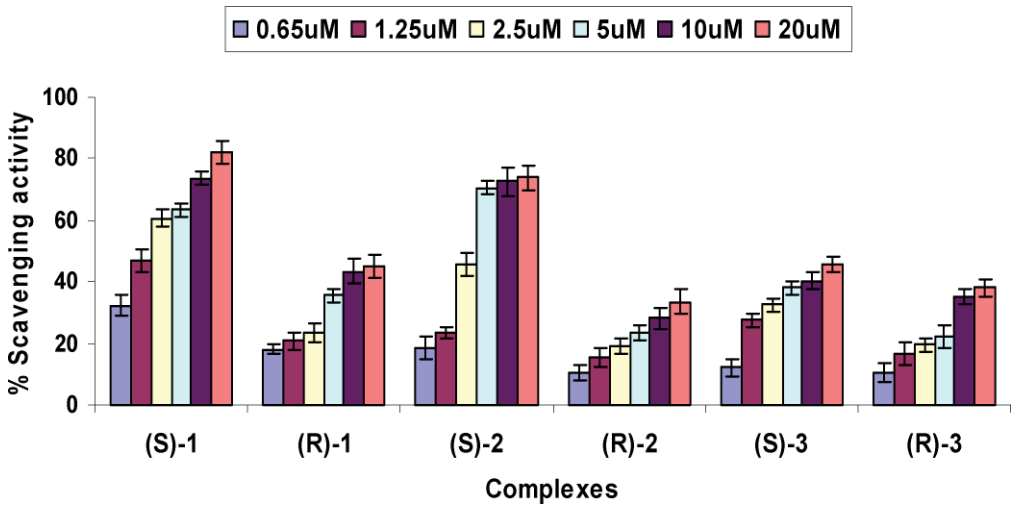

Fig. 15 Scavenging effect of reactive oxygen species in H_2O_2 system by chiral Mn(III) salen complexes.

study have also shown stronger DNA binding ability than their ***R*** enantiomers.

Conclusion

Chiral Mn(III) salen complexes ***S*-1**, ***R*-1**, ***S*-2**, ***R*-2**, ***S*-3** and ***R*-3** having different substituents at the 3,3′ and 5,5′ positions of the salen unit were prepared and characterized by appropriate physico-chemical methods. Binding of these complexes to CT-DNA was investigated by electronic absorption titrations, competitive binding experiments, circular dichroism, thermal denaturation and viscosity measurement studies. Complexes with polar groups at the 5,5′ positions of the salen unit interact with DNA more strongly than those with hydrophobic groups at these positions. Among all the chiral Mn(III) salen complexes, complex ***S*-1** demonstrated highest DNA binding affinity as well as antioxidant activities.

Experimental

Materials and methods

Calf thymus DNA (CT-DNA), 1*S*,2*S*-(+)-cyclohexanediamine and 1*R*,2*R*-(–)-cyclohexanediamine, NBT (Nitroblue-tetrazolium) were purchased from Sigma Aldrich and used as received. EB (ethidium bromide), Riboflavin (vitamin B_2), MET (L-methionine) and DPPH (1,1-diphenyl-picrylhydrazyl) were purchased from S D Fine Chemicals. A solution of CT-DNA in phosphate buffer gave a ratio of UV absorbance at 260 and 280 nm of *ca.* 1.8–1.9, indicating that the DNA was sufficiently free of protein.[45,11] DNA concentration per nucleotide was determined by absorption spectroscopy using the molar absorption coefficient (6600 M^{-1} cm^{-1}) at 260 nm. Commercial grade solvents were distilled before use for the preparation of complexes, ligands and their intermediates. Elemental analysis of complexes was done on a CHNS Analyzer, Perkin Elmer model 2400 (USA). FTIR spectra were recorded by Perkin Elmer Spectrum GX spectrophotometer (USA) in KBr window. NMR spectra were recorded on a Bruker F113V spectrometer (500 MHz, Switzerland) and were referenced internally with TMS. High resolution mass spectra were recorded on a LC-MS (USA) (Q-TOF) LC (Waters), MS (Micromass) instruments using acetonitrile as mobile phase. The spray voltage, tube lens offset, capillary voltage and capillary temperature were set at 4.50 kV, 30.00 V, 23.00 V and 200 °C, respectively, and the *m*/*z* values were quoted for the major peaks in the isotope distribution. UV-vis. and fluorescence spectra were recorded on Shimadzu UV 3101 PC NIR spectrophotometer (Japan) and LS 50B Perkin Elmer luminescence spectrophotometer (USA), respectively. Circular dichroism (CD) spectra were measured on J-815 CD spectrophotometer (Japan). Chiral Mn(III) salen complexes ***S*-1**, ***R*-1**, ***S*-2**, ***R*-2**, ***S*-3** and ***R*-3** were prepared from reaction of the respective chiral ligands, *viz.*, (1*S*,2*S*)-*N*,*N*′-bis-[3-*tert*-butyl-5-chloromethyl-salicylidine]-1,2-cyclohexanediamine ***S*-1′**/(1*R*,2*R*)-*N*,*N*′-bis-[3-*tert*-butyl-5-chloromethyl-salicylidine]-1,2-cyclohexanediamine ***R*-1′**/(1*S*,2*S*)-*N*,*N*′-bis-[3-*tert*-butyl-5-*N*,*N*′*N*′triethylaminomethyl-salicylidine]-1,2-cyclohexanediamine dichloride ***S*-2′**/(1*R*,2*R*)-*N*,*N*′-bis-[3-*tert*-butyl-5-*N*,*N*′*N*′triethylaminomethyl-salicylidine]-1,2-cyclohexanediamine dichloride ***R*-2′**/(1*S*,2*S*)-*N*,*N*′-bis-[3,5-di-*tert*-butylsalicylidene]-1,2-cyclohexanediamine ***S*-3′** and (1*R*,2*R*)-*N*,*N*′-bis-[3,5-di-*tert*-butyl-salicylidene]-1,2-cyclohexanediamine ***R*-3′** with manganese acetate (Scheme 1) according to reported procedure.[30–33]

The characterization data of the complexes are as follows:

(1*S*,2*S*)-*N*,*N*′-bis-[3-*tert*-butyl-5-chloromethyl-salicylidine]-1,2-cyclohexanediaminato manganese(III)chloride *S*-1/(1*R*,2*R*)-*N*,*N*′-bis-[3-*tert*-butyl-5-chloromethyl-salicylidine]-1,2-cyclohexanediaminato manganese(III)chloride *R*-1. ***S*-1**: 70% yield; IR (KBr): 3437, 2942, 2864, 1610, 1533, 1431, 1339, 1308, 1239, 1177, 1027, 888, 821, 779, 731, 644, 566 cm^{-1}; Anal. Calcd. for $C_{30}H_{38}N_2O_2Cl_3Mn$: C, 58.12; H, 6.18; N, 4.52. Found: C, 57.92; H, 6.09; N, 4.42; MS (EI); *m*/*z*: 620.35 [M^+]; UV. Vis. λ_{max} 318(8156), 400 (3610) nm.

***R*-1**: 68% yield; IR (KBr): 3433, 2948, 2868, 1612, 1530, 1432, 1341, 1311, 1241, 1177, 1029, 889, 825, 780, 734, 644, 570 cm^{-1}; Anal. Calcd. for $C_{30}H_{38}N_2O_2Cl_3Mn$: C, 58.12; H, 6.18; N, 4.52. Found: C, 57.88; H, 6.11; N, 4.49; MS (EI); *m*/*z*: 619.95 [M^+]; UV.Vis. λ_{max} 318(13760), 400 (5680) nm.

(1*S*,2*S*)-*N*,*N*′-bis-[3-*tert*-butyl-5-*N*,*N*′*N*′-triethylaminomethyl-salicylidine]-1,2-cyclohexanediaminato manganese(III) trichloride *S*-2/(1*R*,2*R*)-*N*,*N*′-bis-[3-*tert*-butyl-5-*N*,*N*′*N*′triethylamino-methyl-salicylidine]-1,2-cyclohexanediaminato manganese(III) trichloride *R*-2. ***S*-2**: 90% yield; IR (KBr): 3431, 2952, 2865, 1796, 1717, 1613, 1541, 1435, 1388, 1341, 1309, 1267, 1237, 1204, 1169, 1095, 1029, 940, 867, 827, 781, 735, 658, 567, 482 cm^{-1}; Anal. Calcd. for $C_{42}H_{68}N_4O_2Cl_3Mn$: C, 61.35; H, 8.28; N, 6.82. Found: C, 61.29; H, 8.22; N, 6.79. MS (EI); *m*/*z*: 823.75 [M^+]; UV.Vis. λ_{max} 325(7170), 411(3422) nm.

***R*-2**: 92% yield; IR (KBr): 3430, 2954, 2863, 1796, 1719, 1612, 1540, 1435, 1385, 1340, 1310, 1265, 1237, 1204, 1171, 1096, 1030, 940, 869, 824, 779, 734, 658, 566, 485 cm^{-1}; Anal. Calcd. for $C_{42}H_{68}N_4O_2Cl_3Mn$: C, 61.35; H, 8.28; N, 6.82. Found: C, 61.41; H, 8.25; N, 6.76. MS (EI); *m*/*z*: 823.38 [M^+]; UV.Vis. λ_{max} 325(6200), 411(3058) nm.

(1*S*,2*S*)-*N*,*N*′-bis-[3,5-di-*tert*-butylsalicylidene]- 1,2-cyclohexanediaminato manganese(III) chloride *S*-3 and (1*R*,2*R*)-*N*,*N*′-bis-[3,5-di-*tert*-butyl-salicylidene]-1,2-cyclohexanediaminato manganese(III) chloride *R*-3. ***S*-3**: 90% yield; IR (KBr): 3482, 2954, 2866, 1613, 1534, 1462, 1433, 1389, 1311, 1249, 1173, 1029, 868, 836, 780, 747, 670, 641, 569 cm^{-1}; Anal. Calcd. for $C_{36}H_{52}N_2O_2ClMn$: C, 68.07; H, 5.58; N, 4.41. Found: C, 67.42; H, 5.69; N, 4.55; MS (EI); *m*/*z*: 635.15 [M^+]; UV.Vis. λ_{max} 315(12720), 415 (5148) nm.

***R*-3**: 91% yield; IR (KBr): 3483, 2954, 2866, 1614, 1534, 1462, 1433, 1388, 1311, 1249, 1172, 1030, 867, 836, 779, 746, 670, 640, 568 cm^{-1}; Anal. Calcd. for $C_{36}H_{52}N_2O_2ClMn$: C, 68.07; H, 5.58; N, 4.41. Found: C, 67.48; H, 5.64; N, 4.49. MS (EI); *m*/*z*: 634.95 [M^+]; UV.Vis. λ_{max} 315(13270), 415 (5428) nm.

DNA binding and antioxidant activity

Electronic absorption spectroscopy. In order to evaluate the quantitative DNA binding affinity with chiral Mn(III) salen complexes ***S*-1**, ***R*-1**, ***S*-2**, ***R*-2**, ***S*-3** and ***R*-3**, the intrinsic binding constant was obtained by an absorption spectroscopy method. Initially, 1000 μL solution of blank buffer (1 mM phosphate buffer, pH 7.0) was placed in the reference cell and the respective chiral Mn(III) salen complex solution (50 μM) in phosphate buffer having 0.01% DMSO in sample cuvettes (1 cm path length), and the spectra were recorded at 280–450 nm. The incremental concentration of buffered DNA solution (0–300 μM) was added to a fixed concentration of chiral Mn(III) salen complexes ***S*-1**, ***S*-2**, ***S*-3**, ***R*-1**, ***R*-2** and ***R*-3** and spectra were recorded.

The DNA competitive binding study with EB was carried out in phosphate buffer (1 mM, pH 7.0) by keeping a fixed concentration of EB (30 μM) and DNA (100 μM), and different concentrations of chiral Mn(III) salen complexes ***S*-1**, ***R*-1**, ***S*-2**, ***R*-2**, ***S*-3** and ***R*-3** (0–110 μM). The emission spectra were recorded at 500–700 nm, where the excitation wavelength was kept at 478 nm.

Determination of the affinity of chiral enantiomers' interaction with the DNA helix was carried out by circular dichroism spectroscopy (CD). The CD spectra were recorded for the fixed concentration of chiral Mn(III) salen complexes ***S*-1**, ***R*-1**, ***S*-2**, ***R*-2**, ***S*-3** and ***R*-3** (50 μM) in the absence and presence of DNA (0.2 mM) at room temperature on a Jasco J-815 spectrometer at a scanning speed of 50 nm min^{-1}.

Viscosity measurements were performed on Ostwald's viscometer at 30 ± 0.01 °C by using fixed a concentration of DNA solution (50 μM) and increasing the concentration of chiral Mn(III) salen complexes ***S*-1**, ***R*-1**, ***S*-2**, ***R*-2**, ***S*-3** and ***R*-3** (0–60 μM) in phosphate buffer (1 mM, pH 7.0). Each sample was measured in triplicate and the average flow time was calculated with a digital stopwatch. Data were presented as $(\eta/\eta_0)^{1/3}$ *vs.* ([Mn]/[DNA]), where η is the viscosity of DNA in the presence of the complex, and η_0 is the viscosity of DNA alone.[46]

To determine the stability of DNA, thermal denaturation experiments were performed on a TCC 260 temperature controller programmer UV-3101 PC spectrophotometer by mixing solutions of ***S*-1**, ***R*-1**, ***S*-2**, ***R*-2**, ***S*-3** and ***R*-3** (20 μM) in phosphate buffer (1 mM, pH 7.0) with a solution of CT-DNA (0.4 mM). The resulting solutions were incubated for 2 min at different temperatures (35–95 °C) and the absorption intensity was recorded at 260 nm. The T_m value was determined from the graph at the midpoint of temperature curve.

Antioxidant activity

The superoxide radical was generated in the test system by using NBT/VitB_2/MET, and determined spectrometrically by the Nitroblue tetrazolium photoreduction method with a minor modification.[2,17] The suppression of superoxide radical was calculated by measuring the absorbance at 560 nm. Accordingly, the test compounds (chiral Mn(III) salen complexes ***S*-1**, ***R*-1**, ***S*-2**, ***R*-2**, ***S*-3** and ***R*-3**; 0.65–20 μM) were dissolved in 0.01% DMSO and phosphate buffer (1 mM, pH 7.0) and the resulting solution were added to a mixture containing NBT (65 μM), L-MET (13 mM), VitB_2 (1.5 μM), EDTA (0.1 mM) and phosphate buffer (10 mM, pH 7.0). The above mixture was illuminated with a white fluorescence lamp (15 W) for 15 min and its absorbance (A_i) was measured at 560 nm. The above mixture without the test compounds was used as the control and its absorbance under the same conditions was taken as A_0. All the experiments were conducted in triplicate and data were expressed as mean and standard deviation. The suppression ratio was calculated by using the following equation.

$$O_2^{\bullet-} \text{ scavenging activity } (\%) = [(A_0 - A_i)/A_0 \times 100] \quad (3)$$

DPPH radical scavenging activity

The determination of the DPPH scavenging activity was carried out by using a methanolic solution of DPPH (25 mg L^{-1}) mixed with different concentrations (0.65–20 μM) of chiral Mn(III) salen complexes ***S*-1**, ***R*-1**, ***S*-2**, ***R*-2**, ***S*-3** and ***R*-3** in methanol. The above mixture was stirred vigorously for 5 min and was allowed to stand for 1 h at room temperature before its absorbance was measured at 517 nm.[47] The percentage of radical activity was calculated by using following equation.

$$\text{DPPH scavenging activity } (\%) = [(A_0 - A_i)/A_0 \times 100] \quad (4)$$

Scavenging reactive oxygen species in H_2O_2 systems

The H_2O_2 scavenging activity of chiral Mn(III) salen complexes ***S*-1**, ***R*-1**, ***S*-2**, ***R*-2**, ***S*-3** and ***R*-3** was studied according to the slightly modified method of Mohsen *et al.*[48] Thus, H_2O_2 (10 mmol, 5 μL)

was mixed with the test chiral Mn(III) salen complex (0.65–20 μM) in phosphate buffer (10 mM, pH 7.0) and incubated at 37 °C for 19 min. The unreacted H_2O_2 was determined by measuring the absorbance of the reaction mixture at 230 nm. The absorbance obtained without the addition of H_2O_2 was taken as blank, while the solution without chiral Mn(III) salen complex was used as a control (A_0) and with chiral Mn(III) salen complex was used as a sample (A_i). The percentage of H_2O_2 scavenging activity of these complexes was calculated by using the following equation.

$$H_2O_2 \text{ scavenging activity } (\%) = [(A_0 - A_i)/A_0 \times 100] \quad (5)$$

Acknowledgements

N. H. Khan and N. Pandya are thankful to *Council of Scientific & Industrial Research* (*CSIR*) Net Working Project on Catalysis. M. Kumar thankful to CSIR for awarding senior research fellowship.

References

1 S. K. Teo, W. A. Colburn, W. G. Tracewell, K. A. Kook, D. I. Stirling, M. S. Jaworsky, M. A. Scheffler, S. D. Thomas and O. L. Laskin, *Clin. Pharmacokinet.*, 2004, **43**, 311–327.
2 W. Qian, Y. Zheng-Yin, Q. Gao-Fei and Q. Dong-Dong, *BioMetals*, 2009, **22**, 927–940.
3 S. R. Dalton, S. Glazier, B. Leung, S. Win, C. Megatulski and S. J. N. Burgmayer, *J. Biol. Inorg. Chem.*, 2008, **13**, 1133–1148.
4 Y. T. Sun, S. Y. Bi, D. Q. Song, C. Y. Qiao, D. Mu and H. Q. Zhang, *Sens. Actuators, B*, 2008, **129**, 799–810.
5 Y. Xiong and L. N. Ji, *Coord. Chem. Rev.*, 1999, **185**, 711–733.
6 D. S. Sigman, A. Mazumder and D. M. Perrin, *Chem. Rev.*, 1993, **93**, 2295–2316.
7 E. M. Boon, J. K. Barton, P. I. Pradeepkumar, J. Isaksson, C. Petit and J. Chattopadhyaya, *Angew. Chem., Int. Ed.*, 2002, **41**, 3402–3405.
8 C. Metcalfe and J. A. Thomas, *Chem. Soc. Rev.*, 2003, **32**, 215–224.
9 S. Ray, R. Mohan, J. K. Singh, M. K. Samantaray, M. M. Shaikh, D. Panda and P. Ghosh, *J. Am. Chem. Soc.*, 2007, **129**, 15042–15052.
10 K. Wijaya Mudasir, E. T. Wahyuni, H. Inoue and N. Yoshioka, *Spectrochim. Acta, Part A*, 2007, **66**, 163–170.
11 N. H. Khan, N. Pandya, R. I. Kureshy, S. H. R. Abdi, S. Agrawal, H. C. Bajaj, J. Pandya and A. Gupte, *Spectrochim. Acta, Part A.*, 2009, **74**, 113–119.
12 F. Westerlund, F. Pierard, M. P. Eng, B. Norden and P. Lincoln, *J. Phys. Chem. B*, 2005, **109**, 17327–17332.
13 P. U. Maheswari, V. Rajendiran, M. Palaniandavar, R. Parthasarathi and V. Subramanian, *J. Inorg. Biochem.*, 2006, **100**, 3–17.
14 P. U. Maheswari, V. Rajendiran, H. Stoeckli-Evans and M. Palaniandavar, *Inorg. Chem.*, 2006, **45**, 37–50.
15 N. Yoshioka Mudasir and H. Inoue, *J. Inorg. Biochem.*, 2008, **102**, 1638–1643.
16 R. Vijayalakshmi, M. Kanthimathi, R. Parthsarathi and B. U. Nair, *Bioorg. Med. Chem.*, 2006, **14**, 3300–3306.
17 W. Qian, Y. Zheng-Yin, Q. Gao-Fei and Q. Dong-Dong, *Eur. J. Med. Chem.*, 2009, **44**, 2425–2433.
18 P. Valentao, E. Fernandes, F. Carvalho, P. B. Andrade, R. M. Seabra and M. L. Bastos, *Biol. Pharm. Bull.*, 2002, **25**, 1320–1323.
19 B. Bektasoglu, S. E. Celik, M. Ozyurek, K. Guclu and R. Apak, *Biochem. Biophys. Res. Commun.*, 2006, **345**, 1194–1200.
20 P. Bin, Z. Wen-Hui, Y. Lin, L. Han-Wen and Z. Li, *Transition Met. Chem.*, 2009, **34**, 231–237.
21 X. Zhi-Dong, L. He, W. Min, X. Su-Long, Y. Ming and B. Xian-He, *J. Inorg. Biochem.*, 2002, **92**, 149–155.
22 C. Fengjuan, X. Zhihong, X. Pinxian, L. Xiaohui and Z. Zhengzhi, *Anal. Sci.*, 2009, **25**, 359–363.
23 S. Routier, V. Joanny, A. Zaparucha, H. Vezin, J.-P. Catteau, J.-L. Bernier and C. Bailly, *J. Chem. Soc., Perkin Trans. 2*, 1998, 863–868.
24 D. J. Gravert and J. H. Griffin, *Inorg. Chem.*, 1996, **35**, 4837–4847.
25 S. Melvo, S. R. Doctrow, J. A. Schneider, J. Haberson, M. Patel, P. E. Coskun, K. Huffman, D. C. Wallace and B. Malfroy, *J. Neurosci.*, 2001, **21**, 8348–8353.
26 N. H. Khan, S. Agrawal, R. I. Kureshy, S. H. R. Abdi, V. J. Mayani and R. V. Jasra, *Eur. J. Org. Chem.*, 2006, 3175–3180.
27 N. H. Khan, S. Agrawal, R. I. Kureshy, S. H. R. Abdi, K. J. Prathap and R. V. Jasra, *Eur. J. Org. Chem.*, 2008, 4511–4515.
28 R. I. Kureshy, K. J. Prathap, S. Agrawal, M. Kumar, N. H. Khan, S. H. R. Abdi and H. C. Bajaj, *Eur. J. Org. Chem.*, 2009, 2863–2871.
29 R. I. Kureshy, S. Singh, N. H. Khan, S. H. R. Abdi, S. Agrawal and R. V. Jasra, *Tetrahedron: Asymmetry*, 2006, **17**, 2659–2666.
30 T. Rong, Y. Donghong, Y. Ningya, Z. Haihong and Y. Dulin, *J. Catal.*, 2009, **263**, 284–291.
31 R. I. Kureshy, N. H. Khan, S. H. R. Abdi, I. Ahmad, S. Singh and R. V. Jasra, *J. Catal.*, 2004, **221**, 234–240.
32 E. N. Jacobsen, W. Zhang and M. L. Güler, *J. Am. Chem. Soc.*, 1991, **113**, 6703–6704.
33 K. Yu, Z. Gu, R. Ji, L. L. Lou, F. Ding, C. Zhang and S. Liu, *J. Catal.*, 2007, **252**, 312–320.
34 S. Shuo, Y. Tian-Ming, G. Xiao-Ting, J. Ling-Feng, L. jie, Y. Qing-Yuan and J. Liang-Nian, *Chirality*, 2009, **21**, 276–283.
35 N. Chitrapriya, V. Mahalingam, F. R. Fronczek and K. Natarajan, *Polyhedron*, 2008, **27**, 939–946.
36 M. Chauhan and F. Arjmand, *Chem. Biodiversity*, 2006, **3**, 660–676.
37 P. K. Sasmal, A. K. Patra and A. R. Chakravarty, *J. Inorg. Biochem.*, 2008, **102**, 1463–1472.
38 R. M. S. Pereira, N. E. D. Andrades, N. Paulino, A. C. H. F. Sawaya, M. N. Eberlin, M. C. Marcucci, G. M. Favero, E. M. Novak and S. P. Bydlowski, *Molecules*, 2007, **12**, 1352–1366.
39 S. R. Doctrow, K. Huffman, C. B. Marcus, G. Tocco, E. Malfroy, C. A. Adinolfi, H. Kruk, K. Baker, N. Lazarowych, J. Mascarenhas and B. Malfroy, *J. Med. Chem.*, 2002, **45**, 4549–4558.
40 M. Baudry, S. Etienne, A. Bruce, M. Palucki, E. Jacobsen and B. Malfroy, *Biochem. Biophys. Res. Commun.*, 1993, **192**, 964–968.
41 V. Lanza and G. Vecchio, *J. Inorg. Biochem.*, 2009, **103**, 381–388.
42 G. Jian, W. Kai-Ju, N. Jia and Z. Ju-Zhou, *Synthesis and Reactivity in Inorganic, Metal–Organic, and Nano-Metal Chemistry*, 2008, **38**, 562–566.
43 P. Wonchoul and L. Dongyeol, *Bioorg. Med. Chem. Lett.*, 2009, **19**, 614–617.
44 K. serbest, A. Colak, S. Guner and S. karabocek, *Transition Met. Chem.*, 2001, **26**, 625–629.
45 C. Lan-Mei, L. Jie, C. Jin-Can, T. Cai-Ping, S. Shuo, Z. Kang-Cheng and J. Liang-Nian, *J. Inorg. Biochem.*, 2008, **102**, 330–341.
46 M. C. Prabhakara, B. Basavaraju and H. S. Bhojya Naik, *Bioinorg. Chem. Appl.*, 2007, **2007**, 1–7.
47 E. Pontiki, D. Hadjipavlou-Litina and A. T. Chaviara, *J. Enzyme Inhib. Med. Chem.*, 2008, **23**, 1011–1017.
48 Mohsen Mohammadi and Razieh Yazdanparast, *Food Chem. Toxicol.*, 2009, **47**, 716–721.